Progress report: Development of assessment and predictive metrics for quantitative imaging in chest CT
Subaward No: HHSN268201000050C (4a)
PI: Ehsan Samei
Reporting Period: months 7-9

Executive Summary for months 7-9:

The project has achieved the development of a robust modeling framework to predict volumetric performance of a CT scanner from its basic performance characteristics of 2D resolution and noise. Methods have also been developed to measure those characteristics using the ACR as well as a newly-designed phantom that accounts for the influence of patient size, mA modulation, and feature contrast. In this period, the work has been extended to make the model three-dimensional and refine the e' estimation technique. The final stand of this project will focus on generalizing e' to multiple volumetry operators, and to define a standard recipe for quantitative conformance.

Work to be Presented:

Chen B, Samei E. Development of a phantom-based methodology for the assessment of quantification performance. Feb. 2013, *SPIE Medical Imaging*.

Deliverables:

1. ***Deployment of a framework for drawing a correspondence between simple figure of merits (FOM) and quantitative imaging performance in CT.***

   The definition of the framework has been extended from 2D to 3D to since our last report to reflect the impact of slice thickness on volume quantification. This required acquisitions of 3D TTF, 3D NPS, and 3D task function. The acquisition of 3D TTF has been the most challenging part, and was achieved via separate measurements of TTF in XOY-plane and along Z direction, as shown in Figure 1.

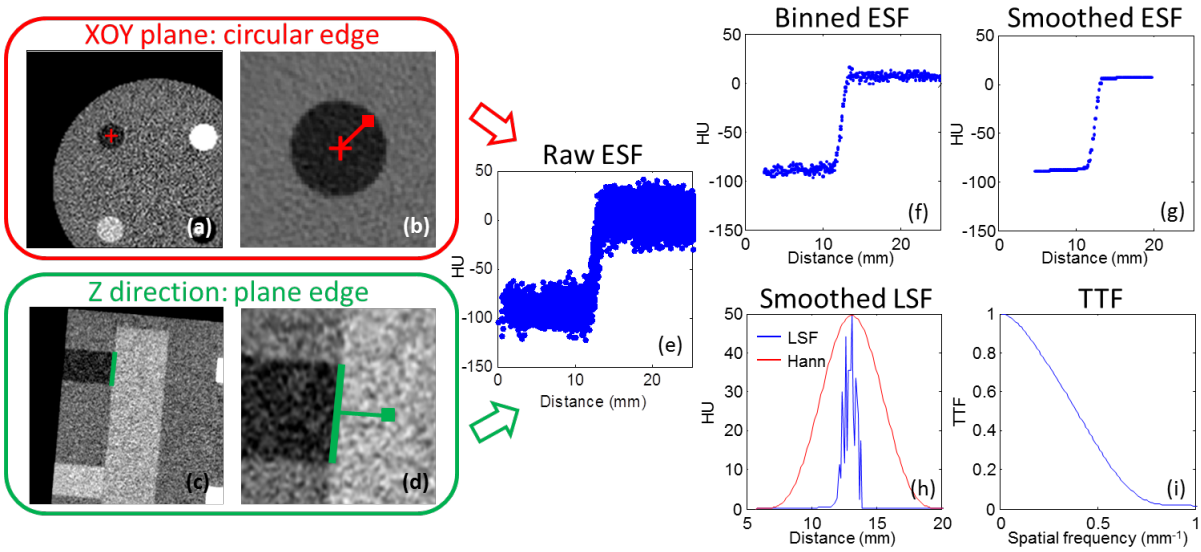

Figure 1: (a,b) The TTF in XOY-plane is calculated with the circular edge of the insert, from which the edge spread function (ESF) can be formed by plotting the intensity of all pixels within the ROI against their distance from the center of the insert. (c,d) The TTF along the z-direction is calculated with the angled plane edge at the end of the insert, from which the ESF can be formed by plotting the intensity of all pixels within the ROI against their distance from the edge. (e,f,g,h,i) The same technique was applied to acquire XOY- or z-TTF from the ESF through a series of de-noise processing.

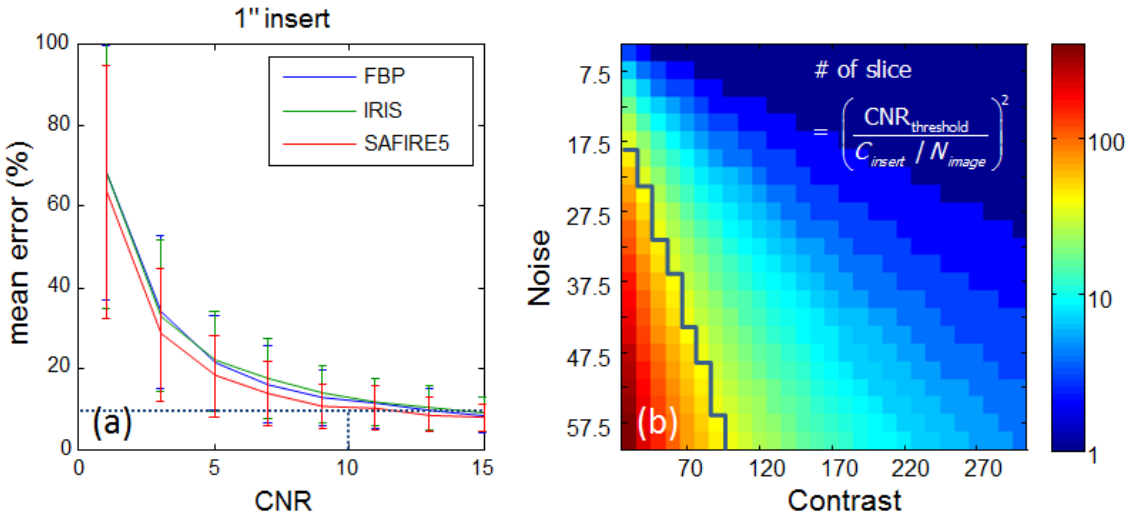

Figure 2: (a) Accuracy and precision of our TTF measuring technique as a function of insert CNR and reconstruction technique. (b) The number of slices required to achieve a CNR of 10 for robust TTF measurement.

Furthermore, the aforementioned TTF measuring technique was validated for its accuracy and precision via simulations. As shown in Figure 2(a), we found a minimum requirement of 10 for the ratio of insert contrast to background noise (CNR) to achieve robust TTF measurement. For inserts of low contrast and protocols of high noise, this CNR requirement was fulfilled by averaging multiple slices, with the number of slices required specified in Figure 2(b).

Finally, we developed a new internal noise term N_i to emulate the fluctuation of the segmentation software due to the difference in placing random seeds. With all the changes mentioned above incorporated, the new 3D e' with internal noise was calculated as

$$e'^2 = \frac{\left[\iiint TTF^2(u,v,w;C,N)\cdot\left|W_{task}(u,v,w)\right|^2 dudvdw\right]^2}{\iiint[NPS(u,v,w;N)+N_i(u,v,w)]\cdot\left|W_{task}(u,v,w)\right|^2 dudvdw}. \quad (1)$$

The new e' model was validated against empirical precision (PRC) measured for 9.5 mm acrylic nodules under 45 protocols, including 5 dose levels (10, 25, 50, 75, and 100% of 7.5 mGy), 3 reconstruction algorithms (FBP and 2 iterative reconstructions, ASIR, and MBIR), and 3 slice thicknesses (0.625, 1.25, and 2.5 mm). As shown in Figure 3, our e' values correlate strongly with the empirical precision values, with linearizable relationships established between the two within the range of this study.

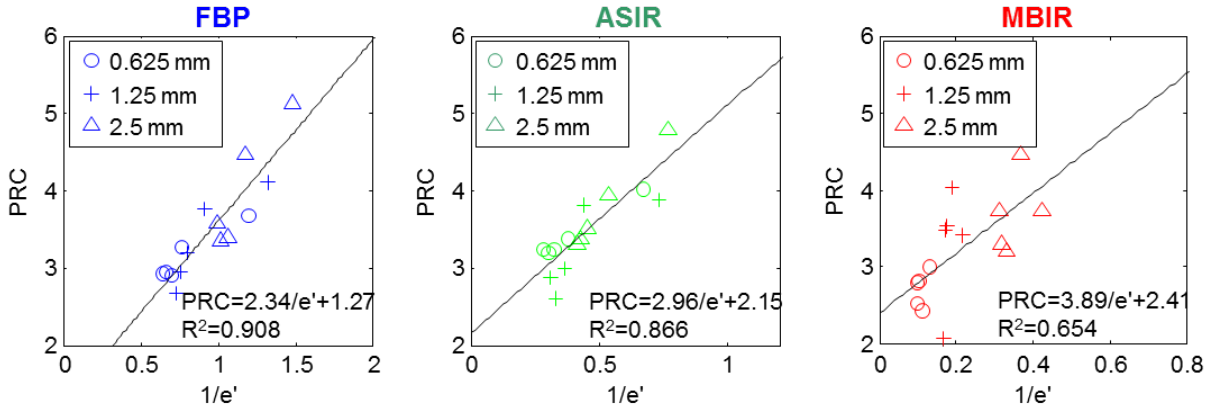

Figure 3: The modified e' still strongly correlates with the empirical precision of volume quantification (PRC).

2. *Table of strengths and weakness of current phantoms for assessing quantitative imaging performance.*

Table 1 summarized the strength and weakness of ACR and Mercury Phantoms in assessing 3D FOMs for quantification precision. The strengths are color-coded in green and the

weaknesses are coded in red. Overall, Mercury Phantom has more strengths than ACR Phantom, but still has space for future improvements.

Table 1: Strengths and weakness of ACR and Mercury Phantoms in assessing quantification precision.

	ACR Phantom	Mercury Phantom
TTF measurement	The four 1'' inserts only provide three contrast levels (air and bone inserts have similar absolute contrast), not sufficient to characterize the entire operating space.	The four 1'' inserts provide two high and two low contrast levels. The four ½'' inserts provide additional low-to-medium contrast levels to help characterize the operating space.
	The circular edges at the side of the cylindrical inserts are perfectly glued with the rest of the phantom, leaving no air gap in between.	Occasional air gap were observed between the insert and the phantom body, which can be eliminated by improving manufacture in future.
	The plane edges at the two ends of the cylindrical insert are not fully polished for TTF measurements along the axial direction.	The plane edge is fully polished for TTF measurements along the axial direction.
	High contrast wedges in between of inserts affect the sharpness of the edge to unknown extent.	No unnecessary components except a low contrast, thin rod in the center of the phantom to combine all sections.
NPS measurement	Only one size (20 cm)	Four sizes (16, 23, 30, and 37 cm) to capture the impact of patient size on noise texture and magnitude.
	High contrast BBs affect the image uniformity to an unknown extent	Most region is uniform except a low contrast, thin rod in the center of the phantom to combine all sections.
Phantom setup	Light	Heavy
	Compact	Require assembly

3. *Identify tolerances and threshold that CT quantification requires in terms of FOM measured on QA phantoms and recommend guidelines for compliance of quantitation techniques (software and hardware).*

As a summary of previous mentioned methodology, Table 2 showed the steps to predict PRC. Only Phase 1 involves scans of the phantom that characterizes the operating space. PRC of any protocol within the operating space characterized in Phase 1 can be calculated in Phase 2, with respect to the nodule characteristics and the segmentation software of interest.

Table 2: Guideline for phantom-based assessment of quantification precision for given combinations of protocol, nodule characteristic, and segmentation software.

Phase 1	**Step 1**	ACR/Mercury Phantom or equivalent that contains - cylindrical inserts of various attenuations for 3D TTF measurements - uniform region for 3D NPS measurements Scan the phantom with a range of dose levels and reconstruct it with multiple slice thicknesses and reconstruction algorithms to compute a library of 3D TTF and NPS values that characterize the entire operating space
Phase 2	**Step 2**	Model W_{task} according to the size, shape, and contrast of the nodule being assessed Model N_i according to the quantification software being assessed
	Step 3	Interpolate a 3D *TTF* from the library built in Step 1 with respect to the nodule's contrast and the image noise of the protocol (imaging and reconstruction parameters) being assessed. This is especially important for protocols involving iterative reconstructions. Interpolate a 3D NPS from the library with respect to the image noise of the protocol
	Step 4	Incorporate *TTF*, *NPS*, W_{task} and N_i into calculating e' for the aforementioned combination of nodule, segmentation software, and protocol
	Step 5	Relate e' to PRC PRC = 2.34/e'+1.27 (FBP) PRC = 2.96/e'+2.15 (ASIR) PRC = 3.89/e'+2.41 (MBIR) Finally, compare PRC to a threshold level and make suggestions

As a demonstration of our e' model's utility in guiding compliance of quantitation techniques, we predicted the PRC of 4.8 mm nodules under a range of protocols, as shown in Figure 4. The PRC values were further compared to a threshold level, 5% in this case. Results show that the quantification of 4.8 mm nodules with FBP reconstruction requires a slice thickness thinner than or equal to 1.25 mm, and a dose higher than or equal to 3.8 mGy.

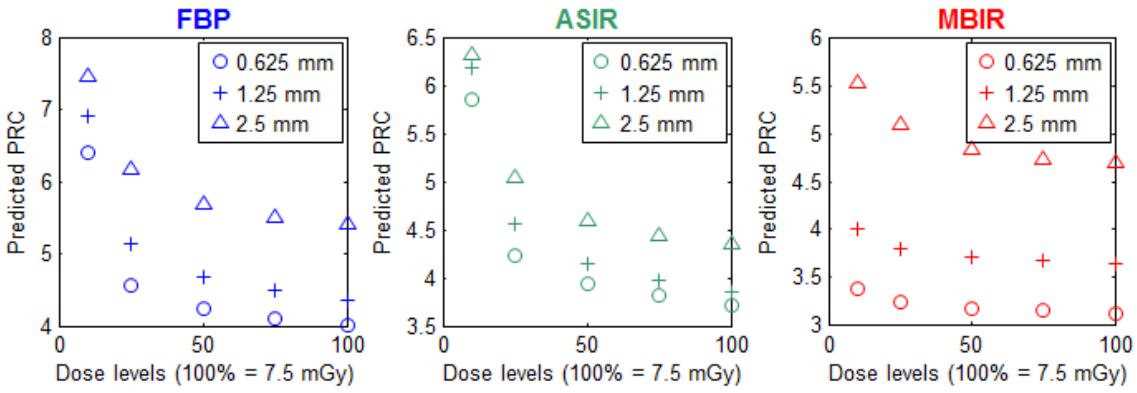

Figure 4: PRC values predicted for 4.8 mm nodule from our e' model.

Work in the coming period

Extend the work to multiple volume estimators.

Define a standard recipe for quantitative conformance.

For various imaging and reconstruction parameters, establish a look-up table for the minimum dose required to achieve a threshold precision.